Published in IET Microwaves, Antennas & Propagation
Received on 12th March 2013
Revised on 27th August 2013
Accepted on 11th October 2013
doi: 10.1049/iet-map.2013.0380

ISSN 1751-8725

Low-phase noise oscillator utilising high-*Q* active resonator based on substrate integrated waveguide technique

Zhe Chen, Wei Hong, Ji Xin Chen, Jianyi Zhou, Lin Sheng Li

State Key Laboratory of Millimeter Waves, Department of Radio Engineering, School of Information Science and Engineering, Southeast University, A3 Building, CNV, 9# Mozhou Eastern Road, Nanjing 211111, People's Republic of China
E-mail: zhechen@emfield.org

Abstract: An X-band low-phase noise planar oscillator employing the substrate integrated waveguide (SIW) active resonator is demonstrated. By compensating the losses in the SIW cavity with an active feedback loop, the *Q*-factor of the SIW active resonator is greatly improved. The measured results show a loaded *Q*-factor of 1569 and unloaded *Q*-factor of 8782, which is very high among other planar resonators. A simplified generalised phase noise condition and its optimisation approach are proposed for the low-phase noise oscillator design. To validate the proposed optimisation approach, experimental prototypes of oscillators using different design parameters and resonators are fabricated. The measured results show that the optimised SIW active resonator oscillator possesses low-phase noise of −109.2 dBc/Hz at 100 kHz at X-band, which is 17 and 9 dB better than the microstrip resonator oscillator and SIW passive resonator oscillator, and is comparable with the dielectric resonator oscillator measured in this study.

1 Introduction

Modern communication systems rely on low-phase noise (PN), low-cost oscillators to provide high spectral pure signal sources. Among other parameters of the oscillator, the PN performance has become increasingly important because communication channels have become closer spaced and more heavily loaded [1]. Lots of research works have been reported to reduce the oscillator PN, which mainly focused on increasing the quality (*Q*) factor of the frequency stabilising resonator/filter [2–9]. Among them, the ceramic, dielectric or metal waveguide cavity resonators possess high *Q*-factor, but their three-dimensional (3D) structure and bulky size result in difficulties for hybrid implementation or on-chip realisation. Their expensive manufacture cost also limits mass reproduction. Other planar resonators, such as microstrip resonators, are low cost, compact, easy to be integrated with other circuits and compatible with standard printed circuit board (PCB) process or monolithic microwave integrated circuit (MMIC) techniques. However, the high loss of microstrip line leads to poor *Q*-factor, which limits its performance. Recently, the substrate integrated waveguide (SIW) technique has drawn tremendous attention, for its low cost, low insertion loss, high *Q* and compatible with standard PCB, low-temperature co-fired ceramic process or MMIC technique. Nevertheless, the unloaded *Q*-factor of a passive SIW resonator is limited to several hundred at microwave frequency [10–15].

To circumvent the *Q*-factor limitations and further reduce the oscillator PN, numerous oscillators have utilised active resonators (ARs)/filters [16–21]. The *Q*-factor can be greatly improved through compensating the losses of the passive resonator (PR). Although the oscillator PN was proven successfully reduced in the previous works, some subtle design issues remain to be explored and addressed. Firstly, the passive elements of the AR are mostly based on microstrip technique in the past, which makes the resonator sensitive to cross-coupling or interferences because of the resonator open structure. This can be improved with an SIW AR, which possesses high *Q*-factor and electromagnetic (EM) shielding structure. Secondly, in previous works, the oscillator design and optimisation approach is either based on the non-linear model of the active device [16–18], or on the linear *S*-parameters [22, 23]. The first approach is relatively accurate, and the oscillator performances can be fully predicted. However, the non-linear model is indispensable. For many commercial transistors, which are only provided with linear *S*-parameters, the first approach is not applicable. The linear approach in [22] can be used for the PN optimisation of the loop-feedback oscillator, but is not suitable for the design of negative-resistance oscillator. The method in [23] is complicated to reach the optimised PN conditions (PNCs).

In this paper, the development of a low-PN oscillator utilising an SIW AR and a simplified PN optimisation approach for negative-resistance oscillator design are presented. In Section 2, the SIW AR with a minimum noise

figure is designed using an active feedback loop. As comparison, a microstrip resonator, SIW PR and dielectric resonator (DR) are also designed and fabricated. The measured results show that the SIW AR possesses very high Q-factor as a planar resonator, which is comparable with the DR. In Section 3, four negative-resistance oscillators using different resonators are developed. Based on the S-parameters of the active device, a simplified PN indicator – generalised PNC and its optimisation process has been proposed. To validate the proposed approach, three SIW AR oscillators (AROs) with different design parameters are measured in Section 4, which proves the feasibility of the PNC optimisation approach. Then, PN comparisons between the oscillators using different resonators are provided with detailed measured results.

2 Design and implementation of high-Q SIW AR and other resonators for comparison

2.1 Design of the SIW AR

According to Cassivi *et al.* [11], the propagation property of SIW is similar to the rectangular waveguide, and TE_{10}-like mode is the fundamental mode. For the design of SIW resonator, the following design equations can be utilised to calculate the resonance frequency [11]

$$f_{R(TEm0q)} = \frac{c_0}{2 \cdot \sqrt{\varepsilon_R}} \cdot \sqrt{\left(m/W_{eff}\right)^2 + \left(q/L_{eff}\right)^2} \quad (1)$$

and

$$L_{eff} = L - \frac{D^2}{0.95 \cdot p}, \quad W_{eff} = W - \frac{D^2}{0.95 \cdot p}$$

where D is the diameter of the metallised hole, p is the period between them, and c_0 is the speed of light in vacuum.

Commonly, there are two ways for designing an AR [16–21, 24], coupling a properly designed negative-resistance device, or introducing an active feedback loop to the PR. The latter is the design method in this paper, as shown in Fig. 1. Since the feedback loop contains an active device, special attention should be paid to the noise design of the AR. It is important to minimise the effect of the added-noise introduced by the amplifier. The detailed design procedure for a low-noise lossless AR is described in [18]. Following Morteza Nick's theory, the SIW resonator can be fully loss-compensated with minimum noise degradation when

$$Q_1 = \frac{G^2 - 1}{G^2} \cdot Q_u \quad (2)$$

$$Q_2 = \left(G^2 - 1\right) \cdot Q_u \quad (3)$$

and

$$Q_1 = \frac{k_1^2 50}{\omega_0 L_r}, \quad Q_2 = \frac{k_2^2 50}{\omega_0 L_r}, \quad Q_u = \frac{R_r}{\omega_0 L_r}$$

where R_r, L_r and C_r are the shunt RLC resonator model parameters for the SIW cavity resonator; Z_L is the load impedance; G is the gain of the amplifier, which is coupled to the SIW cavity through transformer model with turns ratio k_1 and k_2. The quality factor Q_1 and Q_2 denote the loading effect because of the gain stage's input and output. Then, the minimum noise figure of the AR is [18]

$$F_{min} = F_{Passive} + \left(\frac{Q_e}{Q_u}\right) \cdot M \quad (4)$$

and

$$M = \frac{F_{Amp} - 1}{1 - 1/G^2}, \quad F_{Passive} = 1 + \frac{Q_e}{2Q_u}$$

where $F_{Passive}$ is the noise figure of the PR, F_{Amp} is the noise figure of the amplifier in the active feedback loop, Q_u and Q_e are the unloaded and external quality factor of the resonator.

From (2) and (3), the optimum coupling coefficients k_1 and k_2 can be found with

$$k_1^2 = \frac{\left(G^2 - 1\right) \cdot R_r}{G^2 \cdot 50} \quad (5)$$

$$k_2^2 = \frac{\left(G^2 - 1\right) \cdot R_r}{50} \quad (6)$$

The active device used in the feedback loop is InGaAs high-electron-mobility transistor (HEMT) MGF4941AL from MITSUBISHI Corporation, which possesses 12.2 dB gain at 11.5 GHz from the datasheet. It should be noted that it is possible for the AR to oscillate if improperly designed. Once the AR oscillates, it will strongly affect the resonator's performance, and degrade the oscillator PN. Thus, the oscillation in the AR must be avoided. Firstly, the design equations in [18] must be strictly followed to avoid

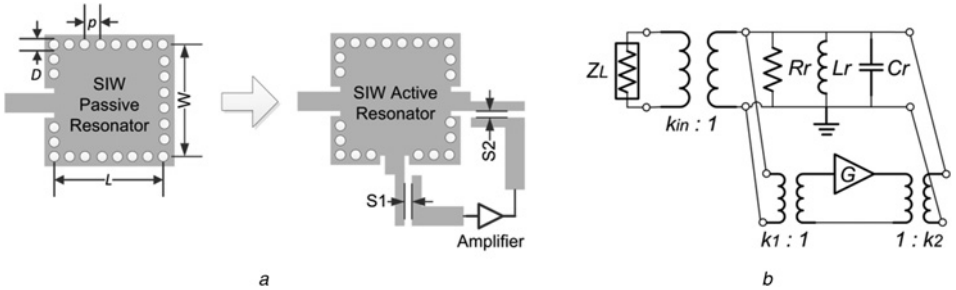

Fig. 1 *Schematic of the SIW AR and its equivalent circuit*

a SIW AR formed by introducing an active feedback loop to the SIW passive resonator
b Equivalent circuit for the SIW AR

doi: 10.1049/iet-map.2013.0380

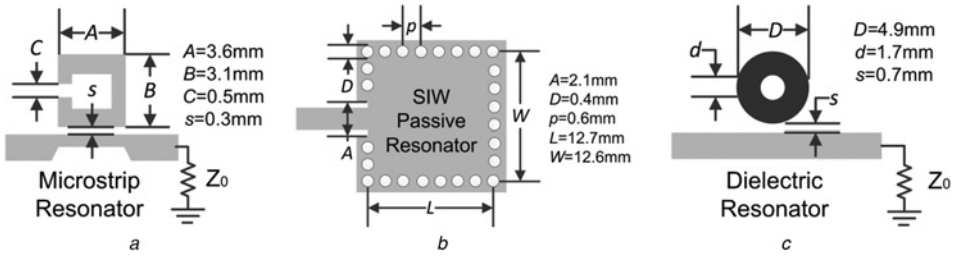

Fig. 2 *Different types of resonators implemented in this paper*

a Microstrip resonator
b SIW PR
c Dielectric resonator

potential oscillation. Secondly, considering the production transistor parameters and PCB fabrication tolerances, a higher gain value of MGF4941AL than the datasheet is utilised for calculating the coupling coefficient k_1 and k_2. For example, we choose $G = 13.2$ dB at 11.5 GHz, which is 1 dB higher than the gain indicated in datasheet. Thus, the calculated coupling coefficients k_1 and k_2 will be a little less than the required values for total loss-compensation. This will ensure that variations in production transistor parameters and passive component tolerances will not cause undesired oscillations in the AR. When the coupling coefficients k_1 and k_2 are found, the dimensions of the coupled microstrip lines, which compose the active loop, can be determined with 3D full-wave simulator Ansoft HFSS. During the simulation and fabrication, Rogers RT/duroid 5880 with dielectric constant of 2.2 and thickness of 0.508 mm is used.

2.2 Implementation and measurement of the SIW AR and other resonators for comparison

The designed SIW AR is fabricated with standard PCB process. For comparison, a passive microstrip resonator, a SIW PR and a DR are also implemented and measured, as shown in Fig. 2. For the microstrip resonator, both electric and magnetic couplings exist [25]. The DR is magnetically coupled to the microstrip line through TE-$_{01\delta}$ mode [26]. All of these resonators are designed to resonate at X-band.

Fig. 3 gives the simulated and measured results for the SIW AR. With biasing voltage $V_{dd} = 2$ V and $I_{dd} = 10$ mA, the losses in the SIW cavity is almost totally compensated with the active feedback loop. Using method provided in [26, 27], the loaded Q-factor Q_l, coupling coefficient k and the unloaded Q-factor Q_u can be calculated with the measured results. Table 1 gives detailed comparison between these different resonators. The measured results show that the SIW AR possesses loaded Q_l of 1569 and unloaded Q_u of 8782 at X-band, which is very high among planar resonators.

3 Design and PN optimisation for SIW AR oscillator and other oscillators

In this section, the design principle of the negative-resistance oscillator is summarised in Section 3.1; then in Section 3.2, a generalised PNC is introduced and utilised for the PN optimisation, based on the S-parameters of the active device. With the proposed PN optimisation approach, four different oscillators are designed and fabricated.

3.1 Design principle of the negative-resistance oscillator

The oscillator design is based on the negative-resistance concept [1]. Series feedback topology is utilised to generate desired negative resistance. The active device used for the oscillator is also MGF4941AL (HEMT). The schematic of the designed SIW ARO is shown in Fig. 4. L_{ser} is the series feedback inductor. R_{bia} is the resistor providing the negative biasing voltage V_{gs} for the HEMT. L is the length of the microstrip line between the transistor and SIW resonator. Through tuning L and L_{ser}, the oscillating conditions can be met: $|\Gamma_{neg}| \cdot |\Gamma_{res}| > 1$ and $\mathrm{Arg}(\Gamma_{neg}) = \mathrm{Arg}(1/\Gamma_{res})$.

For oscillators using other types of resonators, the design procedure is the same as for the SIW ARO. It is the only difference that the SIW AR is replaced by other PRs, as

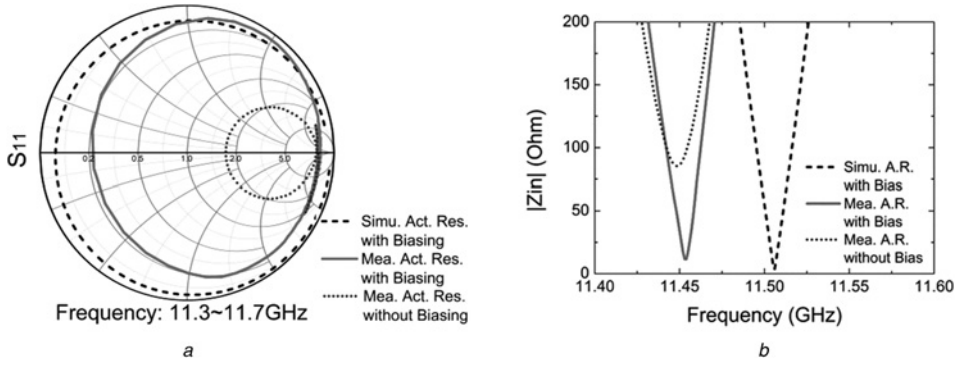

Fig. 3 *Simulated and measured results for the SIW AR*

a S_{11} from 11.3 to 11.7 GHz
b Input impedance magnitude $|Z_{in}|$ of the resonator (Biasing condition for MGF4941AL: $V_{dd} = 2$ V, $I_{dd} = 10$ mA.)

Table 1 Comparison of measured results for different resonators

Resonators	f_{RES}, GHz	$BW_{3\ dB}$, MHz	Loaded Q_L	Unloaded Q_U
microstrip PR[a]	11.762	220	53	139
SIW PR[a]	11.495	40.6	283	562
SIW PR [11]	12.435	—	—	394–542
microstrip AR [17]	9.984	—	548	—
microstrip AR [18]	8	—	720	4000
dielectric resonator [2]	4	—	1500–3800	8000
dielectric resonator[a]	11.281	5.8	1945	9526
SIW AR[b]	11.454	7.3	1569	8782

[a]Other resonators measured in this paper.
[b]The proposed high-Q SIW AR.

shown in Figs. 5*a*–*c*. All the resonators have been designed and measured in Section 2.

Commonly, with the fixed series feedback inductor L_{ser}, a range of L values would satisfy the oscillating conditions. However, the PN performance of the oscillator differs as the L varies. Thus, it is possible to find an optimised L to minimise the oscillator PN.

3.2 Phase noise optimisation by maximising the generalised PNC value

In previous works, to design an oscillator, the widely used approach is based on the non-linear model of the active device [16–18], which is convenient and relatively accurate, and the oscillator performances can be fully predicted, but the non-linear model is indispensable. The second approach relies on the linear S-parameters of the active device [22, 23, 28], which is quite simple and applicable for those commercial transistors with only small-signal S-parameter provided. However, there are still some design issues to be explored for the second approach: in [28], the oscillator design method does not include the PN optimisation process; in [22], the Bode plot can be used for PN optimisation only for the feedback-loop oscillators design and not suitable for the negative-resistance oscillator; in [23], for the negative-resistance oscillator design, the optimum PNCs are summarised as follows:

(i) $\left|(1/\eta)\cdot\left(\left(\mathrm{d}\left(\Gamma_C\right)\right)/(\mathrm{d}\omega)\right)\right|$ is maximised;

(ii) $|(1/\eta)\cdot((\mathrm{d}(\Gamma_D)^{-1})/(\mathrm{d}A))|$ is minimised;

(iii) The reflection coefficients of the resonator locus and the inverse device locus must be orthogonal at the reflection plane;

where Γ_C is the reflection coefficient of the resonator, Γ_D is the reflection coefficient of the active device and η is the magnitude of Γ_C, as shown in Fig. 6*a*. Although the minimum PN can be reached when the above three conditions are satisfied, the second and the third conditions are quite complicated to handle, and cannot be simulated or measured directly.

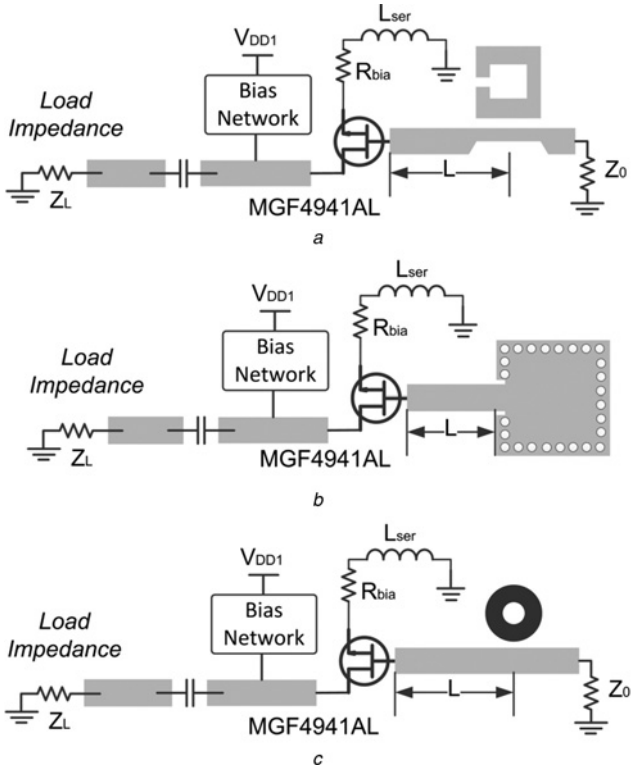

Fig. 5 *Oscillators using other types of PRs in X-band*
a Microstrip PRO
b SIW PRO
c DR oscillator

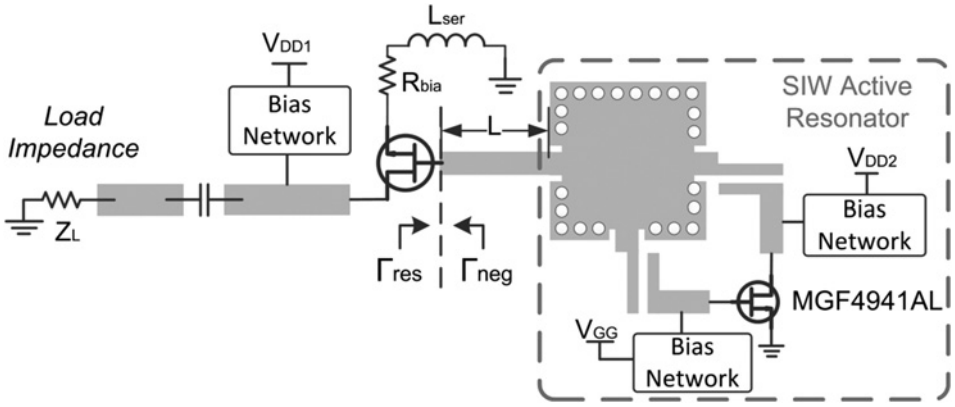

Fig. 4 *Schematic of the proposed oscillator using SIW AR*

doi: 10.1049/iet-map.2013.0380

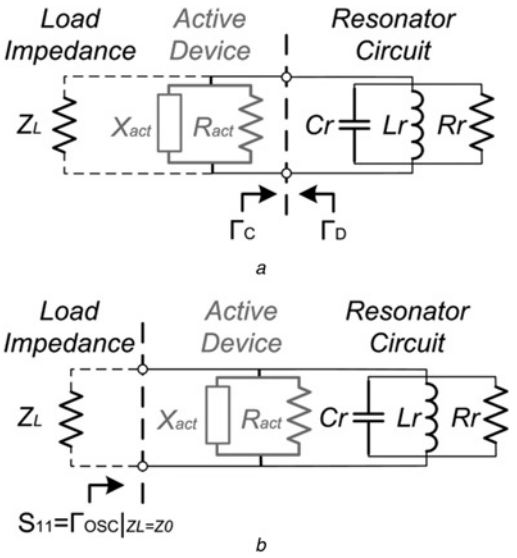

Fig. 6 *Schematics of the oscillator circuit for analysing PNC*

a As in [23], the oscillator is divided into two parts: the active device part and the resonator part, with Γ_C and Γ_D as the optimisation parameters

b Proposed in this paper, the active device is included into the generalised one-port network, with S_{11} as the optimisation parameter

In this paper, a simplified generalised PNC is defined as

$$\mathrm{PNC} = \left|\frac{1}{r}\cdot\frac{\mathrm{d}(S_{11})}{\mathrm{d}\omega}\right| \tag{7}$$

and

$$S_{11} = \Gamma_{\mathrm{OSC}}\big|_{Z_L=Z_0} = r(\omega)\cdot \mathrm{e}^{\mathrm{j}\phi(\omega)} \tag{8}$$

where Γ_{OSC} is the reflection coefficient of the oscillator output port, as shown in Fig. 6*b*. The negative impedance ($R_{\mathrm{act}} + \mathrm{j}X_{\mathrm{act}}$), which is generated by the active device, is desired for oscillating, and will also lead to some resonance frequency shift because of the reactance X_{act}. From Fig. 6*b*, the resonator circuit and the active device are taken as a generalised one-port network, including the effect of both the R_{act} and X_{act}. Thus, the proposed PNC is a proper indicator for the PN performance of the oscillator, and it is easy to be analysed or simulated with commercial software. When PNC is maximised, the optimum PNC can be reached. Compared with the three conditions in [23], the proposed PNC condition is quite simple for optimising the oscillator PN.

Substituting (8) into (7)

$$\mathrm{PNC} = \left|\frac{r'(\omega)}{r(\omega)}\cdot \mathrm{e}^{\mathrm{j}\phi(\omega)} + \mathrm{j}\phi'(\omega)\mathrm{e}^{\mathrm{j}\phi(\omega)}\right| \tag{9}$$

at oscillating frequency ω_0, $\mathrm{e}^{\mathrm{j}\phi(\omega)}\big|_{\omega=\omega_0} = 1$, thus

$$\mathrm{PNC}|_{\omega=\omega_0} = \left|\frac{r'(\omega_0)}{r(\omega_0)} + \mathrm{j}\phi'(\omega_0)\right| \tag{10}$$

From (10), the first part of PNC is dependent on the magnitude of S_{11}, and $\varphi'(\omega_0)$ is the phase slope of S_{11} at oscillating frequency ω_0. Thus, finding optimum design parameter L (the length of the microstrip line between the active device and the resonator circuit) to maximise PNC is the goal of our PN optimisation. Let

$$\mathrm{X} = \left|\frac{r'(\omega_0)}{r(\omega_0)}\right|, \quad \Upsilon = \left|\phi'(\omega_0)\right| \tag{11}$$

then

$$\mathrm{PNC}|_{\omega=\omega_0} = \sqrt{X^2 + Y^2} \tag{12}$$

Thus, a negative-resistance oscillator design can be summarised as this: firstly, using method in [28] to obtain a set of L values (the microstrip length between the active device and the resonator circuit) to satisfy the oscillating conditions; secondly, setting L as the variable, the PNC value can be obtained from S-parameter simulation with advanced design system. According to the peak PNC value, the optimum L can be determined, and a low-PN SIW oscillator can be expected. The utilised MGF4941AL are provided with S-parameters under $V_{\mathrm{d}} = 2$ V, $I_{\mathrm{d}} = 10$ mA.

Table 2 gives the simulated PNC for SIW ARO with these L values. With $L = 10.0$ mm, the maximised PNC of

Table 2 Simulated PNC for the oscillator using SIW AR

L, mm	f_{OSC}, GHz	X ($\times 10^{-6}$)	Y ($\times 10^{-6}$)	PNC ($\times 10^{-6}$)
9.4	11.480	0.142	9.093	9.094
9.6	11.479	0.219	8.368	8.371
9.8	11.479	0.415	12.545	12.552
10.0	11.479	0.122	137.01	137.01
10.2	11.478	0.166	109.47	109.47
10.4	11.479	0.966	26.078	26.096
10.6	11.480	0.141	15.440	15.441

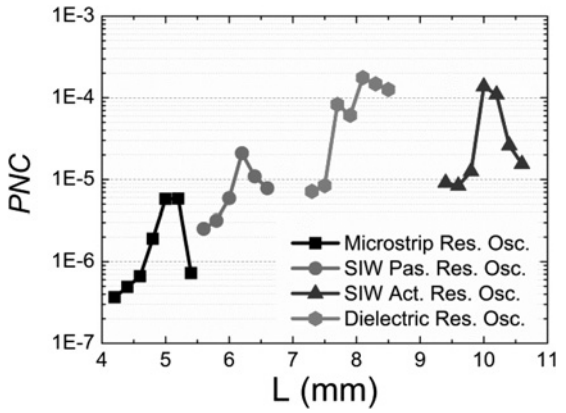

Fig. 7 *Simulated PNC value against L, for the oscillators using different resonators*

Table 3 Optimum L for the oscillators using different resonators

Oscillators	Opt. L, mm	f_{OSC}, GHz	PNC ($\times 10^{-6}$)
microstrip resonator oscillator	5.2	11.891	5.818
SIW PRO	6.2	11.495	20.97
dielectric resonator oscillator	8.3	11.279	176.46
SIW ARO	10.0	11.459	137.01

137.01×10^{-6} can be obtained, which corresponds to the best PN performance. From Table 2, it is worthy noted that $X \ll Y$, thus PNC is mainly dependent on Y, or the phase slope of S_{11} at oscillating frequency. This is similar to the conclusion in [22] for feedback-loop oscillators. Fig. 7 compares the simulated PNC for all of the four oscillators utilising different resonators. It is noted that each of the four curves has a peak PNC value, with which the oscillator can possess optimum PN performance. According to the peak PNC point, the optimum L value can be determined.

Table 3 lists the optimum L values and the peak PNC for each of the four oscillators using different resonators. From Table 3, it is clearly that the PNC of the SIW ARO is much larger than the oscillators using microstrip resonator or SIW PR, and comparable with the PNC of DR oscillator (DRO). Thus, a low-PN SIW ARO can be expected. With the optimum L value, four oscillators utilising different resonators are fabricated through standard PCB process. Fig. 8 shows the pictures of the experimental prototypes. To validate the PNC optimisation approach, two additional SIW AROs with non-optimum L are also fabricated.

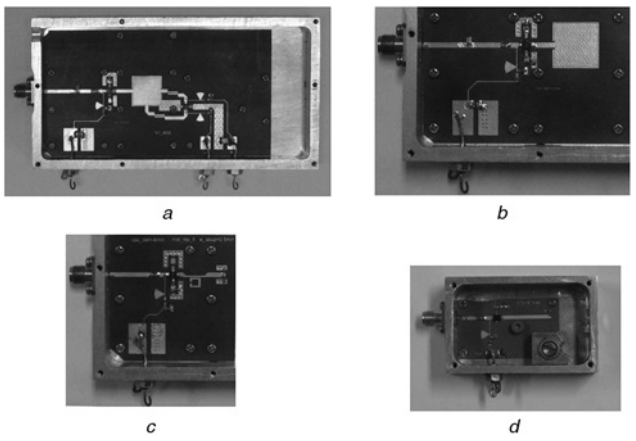

Fig. 8 *Fabricated experimental prototypes of the oscillators using different resonators in X-band*

a SIW ARO
b Microstrip resonator oscillator
c SIW PRO
d DR oscillator

4 Experimental measurement of the implemented oscillators

4.1 Validation of the PNC optimisation approach

To validate the proposed PN optimisation process, three SIW AROs are fabricated and measured. The design parameters are all the same for the three AROs, except that the L of SIW ARO-I is 10.0 mm (the simulated optimum value), whereas L of SIW ARO-II is 9.4 mm, and the L of SIW ARO-III is 10.6 mm (non-optimum value). Fig. 9 shows the measured output spectrums of the three SIW AROs with Agilent signal analyser N9030A. Figs. 9*a* and *b* show the output spectrum for SIW ARO-I. The oscillating frequency is 11.457 GHz with an output power of 2.01 dBm. (Owing to marker resolution limit of N9030A, the oscillating frequency is shown as 11.41 GHz in Fig. 9*a*.) The insertion loss of the connected cable is 2.7 dB, thus the actual output

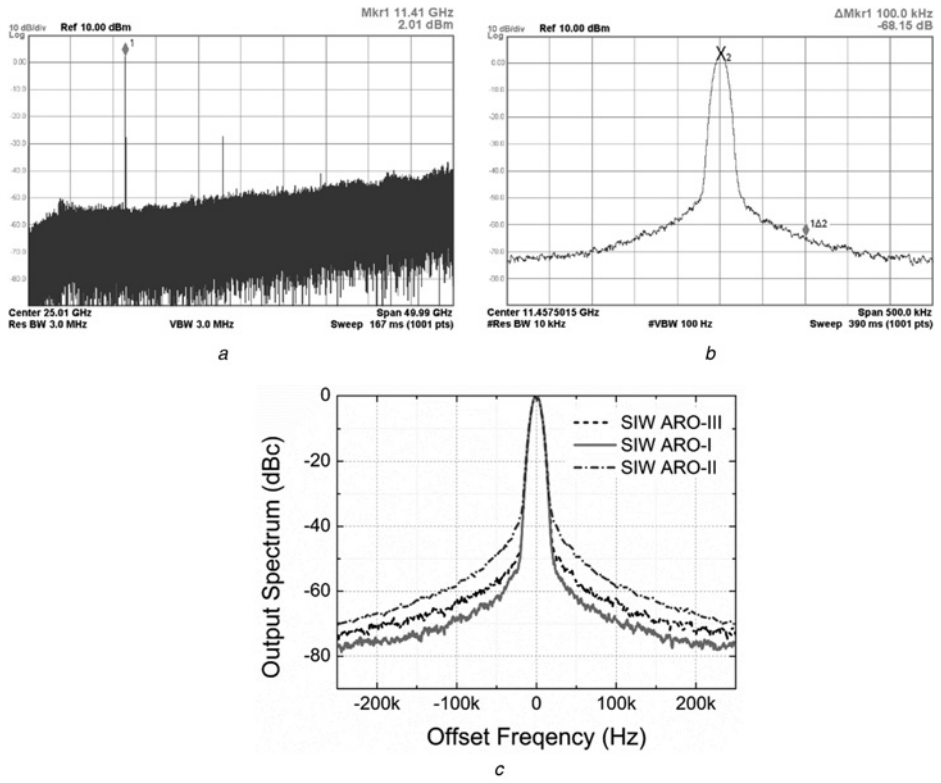

Fig. 9 *Measured results of SIW AROs*

a Output spectrum 10 MHz to 50 GHz for SIW ARO-I (with optimum $L = 10.0$ mm)
b Output spectrum with span of 500 kHz for SIW ARO-I
c Comparison of the output spectrum for SIW ARO-I (with optimum $L_{opt} = 10.0$ mm), ARO-II (with non-optimum $L = 9.4$ mm) and ARO-III (with non-optimum $L = 10.6$ mm); the VBW = 10 kHz

doi: 10.1049/iet-map.2013.0380

power is 4.7 dBm for the oscillator. From Fig. 9*a*, the second harmonic is below −29 dBc and the third harmonic is below −43 dBc. For a free running oscillator, the PN can be calculated with the following relation [12]

$$\mathrm{PN} = P_{\mathrm{SideBand}} - P_{\mathrm{Carrier}} - 10\log_{10}(\mathrm{RBW}) \qquad (13)$$

where P_{Carrier} is the power of the carrier frequency, P_{SideBand} is the power of the sideband noise at the frequency offset and RBW = 10 kHz. Thus, from Fig. 9*b*, the PN of the SIW ARO-I is −108.15 dBc/Hz at 100 kHz offset. Fig. 9*c* shows the PN for the three SIW AROs with a span of 500 kHz, where the output spectrums are centred at the oscillating frequency and normalised to the maximum output power. From Fig. 9*c*, SIW ARO-I has the best PN performance, with 5.3–9.5 dB PN improvement at 100 kHz offset, compared with SIW ARO-II and ARO-III, which do not utilise the optimum L value. It is clearly that maximisation of PNC has successfully optimised the PN of the SIW ARO-I.

For the SIW AR, the consumed DC power is 20 mW, with $V_{\mathrm{dd2}} = 2$ V and $I_{\mathrm{dd2}} = 10$ mA. The DC power for the oscillator itself is 28 mW, with $V_{\mathrm{dd1}} = 2.8$ V and $I_{\mathrm{dd1}} = 10$ mA. Thus, the total DC power for the SIW ARO is 48 mW, corresponding to 6.2% DC-RF conversion efficiency. Some DC power has been consumed on the active device in the SIW AR, and on the biasing resistor R_{bia}. The power conversion efficiency can be improved if non-resistance biasing network and lower quiescent current for MGF4941AL are utilised.

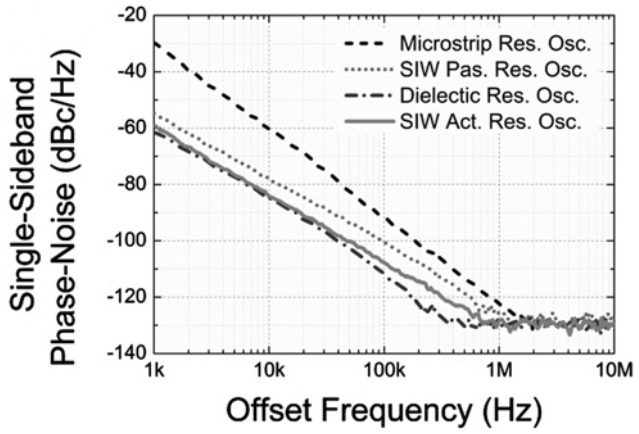

Fig. 10 *Measured PN of the oscillators using different resonators with frequency offset from 1 kHz to 10 MHz, obtained with Rohde and Schwarz source analyser FSUP50*

4.2 Comparison of four oscillators using different resonators

Furthermore, Rohde and Schwarz signal source analyser FSUP50 is utilised to accurately measure the PN performance of the four oscillators (all with optimum L values). Fig. 10 shows the measured results. The PN of the SIW ARO is decreased by 17 and 9 dB at 100 kHz offset, compared with the microstrip PR oscillator (PRO) and the SIW PRO, respectively. At 10 kHz offset, the PN improvement is 23 and 5 dB, respectively. Overall, the PN performance of the SIW ARO is much better than the microstrip PRO or SIW PRO, and is even comparable with the DRO, except for frequency offset between 100 and 600 kHz, where the DRO has 2–7 dB improvement. That is because in Lesson's theory [29, 30], the second PN corner frequency is ($\omega_0/2Q$). And DR has higher Q-factor than the SIW AR, as shown in Table 1. Since the four oscillators utilised the same active device (MGF4941AL), their flicker corner frequencies are the same. Thus the measured PN performances of the four oscillators are mainly dependent on the resonator Q-factor and the PN optimisation process, which coincides with the PNC value in Table 3. This further proved the validity of the proposed PNC optimisation approach.

According to [29], the PN floor is

$$\text{Phase noise floor} = 10\log_{10}\left(\frac{2FkT}{P_{\mathrm{Carrier}}}\right) \qquad (14)$$

where F is the factor of the active device to account for the increased noise in $(1/\Delta f)^2$ region. With (14), the PN floor is only dependent on the active device and the output power level. This has been observed in Fig. 10, where the noise floors of the four oscillators are all around −130 dBc/Hz.

The FOM of an oscillator can be calculated with [18]

$$\mathrm{FOM} = L(\Delta f) - 20\log_{10}\left(\frac{f_0}{\Delta f}\right) + P_{\mathrm{DC}}(\mathrm{dBm}) \qquad (15)$$

where $L(\Delta f)$ is the PN, Δf is the frequency offset, f_0 is the oscillation frequency and P_{DC} is the total consumed DC power. Thus the FOM of the measured SIW ARO is −192.8 dBc/Hz. Performance comparison of oscillators using different active/passive resonators at X-band is listed in Table 4.

Table 4 Comparison of hybrid oscillators at X-band

Device	Resonator	f_{osc}, GHz	L (100 kHz), dBc/Hz	FOM, dBc/Hz
HEMT[a]	microstrip PR	11.87	−92.1	−178.6
Si Bipolar Junction Transistor [3]	microstrip hairpin resonator	9	−109	−185.6
pHEMT [17]	microstrip AR	10	−114.3	−187.4
SiGe Heterojunction Bipolar Transistor [6]	microstrip active filter	8	−125	−205
pHEMT [13]	SIW PR	9.5	−92	−184
HEMT[a]	SIW PR	11.48	−100.3	−186.8
HEMT[a]	dielectric resonator	11.24	−111.6	−198.1
HEMT[b]	SIWAR	11.45	−109.2	−192.8

[a]Other oscillators measured in this paper.
[b]The proposed SIW ARO in this paper.

5 Conclusions

A low-PN oscillator employing SIW AR is presented in this paper. By using an active feedback loop, the loss in the SIW cavity is compensated; thus the Q-factor of the SIW AR is greatly improved. Design method is taken to minimise the effect of the added-noise introduced by the amplifier in the AR. As comparison, a microstrip resonator, a SIW PR and a DR are also implemented and measured. The measured results show a loaded Q-factor of 1569 and an unloaded Q-factor of 8782 for the SIW AR, which is ultra-high among other planar resonators and comparable with the DR. In addition, the planar SIW AR possesses EM shielding structure, making the resonator resistant to the cross-coupling or outside interferences, which is the advantage over the microstrip-type resonator.

During the oscillator design, a novel PN optimisation approach is proposed and utilised by maximising the PNC value. This approach is based on the linear S-parameters of the active device, thus the non-linear model is not required. Compared with the previous PN optimisation approach based on the linear S-parameter, the proposed PNC optimisation approach is quite simple and easy to be analysed or simulated. To validate the proposed approach, experimental prototypes of oscillators using different design parameter L and different resonators are fabricated. The measured results show great PN improvement for the SIW ARO: −83.6 dBc at 10 kHz offset, −109.2 dBc/Hz at 100 kHz offset at X-band, which is comparable with the DRO measured in this paper. The PN improvement is 17 and 9 dB at 100 kHz offset, compared with the microstrip PRO and SIW PRO, respectively.

In addition, by coupling varactor to the SIW cavity [13, 31], a low-PN voltage-controlled oscillator can be expected to be implemented with the developed SIW ARO.

6 Acknowledgment

This work is supported in part by 'the Fundamental Research Funds for the Central Universities' of China, in part by National 973 Project under Grant No. 2010CB327405, in part by NSFC under Grant No. 60921063 and in part by the National High Tech. Project under Grant Nos. 2010ZX03007-002-01 and 2011ZX03004-003, and are sponsored by Qing Lan Project. The authors thank MITSUBISHI Electric for their support in microwave HEMT devices.

7 References

1 Rhea, R.W.: 'Oscillator design and computer simulation' (Noble Publishing Corporation, Atlanta, 1995, 2nd edn.), pp. 111
2 Regis, M., Llopis, O., Graffeuil, J.: 'Nonlinear modeling and design of bipolar transistors ultra-low phase-noise dielectric-resonator oscillators', *IEEE Trans. Microw. Theory Tech.*, 1998, **46**, (10), pp. 1589–1593
3 Dussopt, L., Guillois, D., Rebeiz, G.M.: 'A low phase noise silicon 9 GHz VCO and 18 GHz push-push oscillator'. IEEE MTT-S Int. Microwave Symp. Digest, June 2002, pp. 695–698
4 Choi, J., Mortazawi, A.: 'A new X-band low phase-noise multiple-device oscillator based on the extended-resonance technique', *IEEE Trans. Microw. Theory Tech.*, 2007, **55**, (8), pp. 1642–1648
5 Kawasaki, K., Tanaka, T., Aikawa, M.: 'An octa-push oscillator at V-band', *IEEE Trans. Microw. Theory Tech.*, 2010, **58**, (7), pp. 1696–1702
6 Choi, J., Nick, M., Mortazawi, A.: 'Low phase-noise planar oscillators employing elliptic-response bandpass filters', *IEEE Trans. Microw. Theory Tech.*, 2009, **57**, (8), pp. 1959–1965
7 Llopis, O., Cibiel, G., Kersale, Y., Regis, M., Chaubet, M., Giordano, V.: 'Ultra low phase noise sapphire – SiGe HBT oscillator', *IEEE Microw. Wirel. Compon. Lett.*, 2002, **12**, (5), pp. 157–159
8 Lee, Y.-T., Lim, J.-S., Park, J.-S., Ahn, D., Nam, S.: 'A novel phase noise reduction technique in oscillators using defected ground structure', *IEEE Microw. Wirel. Compon. Lett.*, 2002, **12**, (2), pp. 39–41
9 Lee, W.-C., Lin, S.-C., Tzuang, C.-K.C.: 'Planar realization of low phase noise 15/30 GHz oscillator/doubler using surface mount transistors', *IEEE Microw. Wirel. Compon. Lett.*, 2003, **13**, (1), pp. 10–12
10 Yang, N., Caloz, C., Wu, K.: 'TE210 mode balanced oscillator using substrate integrated waveguide resonator', *IET Microw. Antennas Propag.*, 2011, **5**, (10), pp. 1188–1194
11 Cassivi, Y., Perregrini, L., Wu, K., Conciauro, G.: 'Low-cost and high-Q millimeter-wave resonator using substrate integrated waveguide'. Proc. European Microwave Conf., Milan, Italy, 2002, pp. 1–4
12 Cassivi, Y., Wu, K.: 'Low cost microwave oscillator using substrate integrated waveguide cavity', *IEEE Microw. Wirel. Compon. Lett.*, 2003, **13**, (2), pp. 48–50
13 He, F.F., Wu, K.: 'A low phase-noise VCO using an electronically tunable substrate integrated waveguide resonator', *IEEE Trans. Microw. Theory Tech.*, 2010, **58**, (10), pp. 3452–3458
14 Georgiadis, A., Via, S., Collado, A., Mira, F.: 'Push-push oscillator design based on a substrate integrated waveguide (SIW) resonator'. Proc. European Microwave Conf., Rome, Italy, 2009, pp. 1231–1234
15 Zhong, C., Xu, J., Yu, Z., Zhu, Y.: 'Ka-band substrate integrated waveguide Gunn oscillator', *IEEE Microw. Wirel. Compon. Lett.*, 2008, **18**, (7), pp. 461–463
16 Lee, J., Lee, Y.-T., Nam, S.: 'A phase noise reduction technique in microwave oscillator using high-Q active filter', *IEEE Microw. Wirel. Compon. Lett.*, 2001, **12**, (11), pp. 426–428
17 Lee, Y.-T., Lee, J., Nam, S.: 'High-Q active resonator using amplifiers and their applications to low phase-noise free-running and voltage-controlled oscillators', *IEEE Trans. Microw. Theory Tech.*, 2004, **52**, (11), pp. 2621–2626
18 Nick, M., Mortazawi, A.: 'Low phase-noise planar oscillators based on low-noise active resonators', *IEEE Trans. Microw. Theory Tech.*, 2010, **58**, (12), pp. 1133–1139
19 Rohde, U.L., Poddar, A.K.: 'Active planar coupled resonators replace traditional high Q resonators in low phase noise oscillators/VCOs'. IEEE Radio and Wireless Symp., 2007, pp. 39–42
20 Hwang, M.-S., Oh, S., Koo, J.-J., *et al.*: 'An active resonator using defected ground structure with islands'. Proc. Asia-Pacific Microwave Conf., 2007, pp. 1–4
21 Alinikula, P., Kaunisto, R., Stadius, K.: 'Monolithic active resonators for wireless applications'. IEEE MTT-S Int. Microwave Symp. Digest, 1994, pp. 1151–1154
22 Randall, M., Hock, T.: 'General oscillator characterization using linear open-loop S-parameters', *IEEE Trans. Microw. Theory Tech.*, 2001, **49**, (6), pp. 1094–1100
23 Esdale, D.J., Howes, M.J.: 'A reflection coefficient approach to the design of one-port negative impedance oscillators', *IEEE Trans. Microw. Theory Tech.*, 1981, **29**, (8), pp. 770–776
24 Chen, Z., Hong, W., Chen, J.-X.: '*High-Q planar active resonator based on substrate integrated waveguide technique*', *Electron. Lett.*, 2012, **48**, (10), pp. 575–577
25 Hong, J.-S., Lancaster, M.J.: 'Microstrip filters for RF/microwave applications' (Wiley & Sons, New York, 2001)
26 Khanna, A., Garault, Y.: 'Determination of loaded, unloaded, and external quality factors of a dielectric resonator coupled to a microstrip line', *IEEE Trans. Microw. Theory Tech.*, 1983, **31**, (3), pp. 261–264
27 Pozar, D.M.: 'Microwave engineering' (Wiley & Sons, New York, 1998, 2nd edn.)
28 Dearn, A.: 'How to design RF circuits – oscillators', How to Design RF Circuits, IEE Training Course, 2000
29 Lee, T.H., Hajimiri, A.: 'Oscillator phase noise: a tutorial', *IEEE J. Solid-State Circuits*, 2000, **35**, (3), pp. 326–336
30 Leeson, D.B.: 'A simple model of feedback oscillator noise spectrum'. Proc. IEEE, 1966, 54, (2), pp. 329–330
31 Sirci, S., Martinez, J.D., Taroncher, M., Boria, V.E.: 'Varactor-loaded continuously tunable SIW resonator for reconfigurable filter design'. Forty-first European Microwave Conf., 2011, pp. 436–439